Final Report

CAN NNS06AA05G
NASA VOLCANIC CLOUD DATA FOR AVIATION HAZARDS

Lead Organization: Joint Center for Earth Systems Technology/University of Maryland Baltimore County, Baltimore, MD 21250

Principal Investigator: Dr. Arlin Krueger

Co-Investigators:

Dr. Nickolay Krotkov,	GEST/UMBC
Dr. Kai Yang,	GEST/UMBC
Dr. Simon Carn,	JCET/UMBC ;Michigan Tech Univ. Houghton, MI
Mr. Keith Evans,	JCET/UMBC

NOAA Collaborators

Dr. Gilberto Vicente	NOAA/NESDIS/OSDPD
Mr. George Serafino	NOAA/NESDIS/OSDPD (until 2008)
Dr. Wilfrid Schroeder	ESSIC/UMCP
Mr. Eric Hughes	ESSIC/UMCP

USGS Collaborators

Ms. Marianne Guffanti	Volcanic Hazards Program, Reston, VA

Period of Performance April 2006 – January 2010

Abstract

Volcanic ash clouds are hazardous to aviation. Existing operational ash detection methods using IR brightness temperature differences fail with fresh ash clouds and when water or high clouds mask the signals. The NASA research EOS Aura/Ozone Monitoring Instrument (OMI) is a UV instrument that can detect ash and sulfur dioxide under nearly all daytime conditions. Sulfur dioxide is a proxy for ash from explosive magmatic eruptions. A collaboration, funded by the NASA Applied Sciences Aviation Weather

Program, between the UMBC OMI SO_2 algorithm development group and the NOAA/NESDIS data product development team was formed to produce OMI SO_2 and ash data in near real-time for distribution by NOAA to Decision Support Systems. New algorithms and tools were developed to accurately measure SO_2 and ash in deep volcanic eruption plumes. The large dynamic range of SO_2 retrievals also permitted monitoring of passive emissions from active volcanoes to augment or replace ground-based monitoring systems that are deployed at select volcanoes. The new data allow volcano observatories to judge activity and eruption potential based on emissions over time. Data were provided to operational aviation management agencies for numerous eruptions during the course of the project, including the largest since Pinatubo in 1991, three major eruptions affecting N. Pacific air traffic, numerous low latitude eruptions, and, recently, an eruption in Iceland that shut down air traffic in Europe for days. All were covered with OMI data and used by operational agencies and airline dispatchers for safe flight. A second NRT data stream was set up using MetOp-A GOME-2 morning orbit data that complements the OMI afternoon data.

Summary of Project

Volcanic ash aviation hazards

Volcanic ash is recognized as a serious threat to aircraft in flight. Ash melts at temperatures below the operating temperatures in jet engines, then deposits and solidifies in critical spaces, and can cause engine shut down. In addition erosion of windshields interferes with vision, and deposition in pitot-static probes affects aircraft control. Passenger aircraft have been disabled at high altitudes by fresh ash clouds (< 1 day old) from explosive magmatic eruptions while many more aircraft have been damaged in aging ash clouds. Ash is lofted to high altitudes in explosive magmatic eruption columns to produce a primary risk to flight. Examples are the Kasatochi eruption of 2008 and the Pinatubo eruption of 1991. The volcanic explosion is driven by the expansion of volatile components of the magma, including water and sulfur dioxide. Phreatic (steam-driven) processes from subglacial volcanic vents can produce lower tropospheric fine ash plumes that can travel long distances. The April 2010 eruption of Eyjafjallajokull volcano in Iceland is an extreme example of fine ash created from glacial melt water falling on hot magma affecting air traffic and terminal operations across Europe. Ash settling from high altitude plumes, lofting from pyroclastic flows, and pulverized rock dust from dome collapses and phreatic eruptions are a risk to terminal operations and local aviation.

Deficiencies in current operational ash detection system

Air traffic control agencies and airline flight dispatchers rely on NOAA for information on the time and location of ash clouds. The aviation industry would like detection within 5 minutes of an eruption although no civilian satellite systems exist with this capability. Indirect but very useful information on eruption timing is available with seismic data from those volcanoes equipped with instrumentation. However seismic data cannot help in locating an ash cloud or in determining its height and size.

International Volcanic Ash Advisory Centers (VAAC's) were established for collecting the information needed for this task, analyzing the data, forecasting drift of the volcanic cloud, and preparing NOTAMs and advisory bulletins. forecasting drift of the volcanic cloud, and preparing NOTAMs and advisory bulletins. These organizations depend on dispersion models, operational satellite data, seismic monitors, and volcanic observatories for their information. For example, VAACs in London and Toulouse rely mostly on dispersion models for plume forecasts. London runs a version of the NAME Lagrangian dispersion model (http://www.metoffice.gov.uk/aviation/vaac/eruption_detection.html), while Toulouse (http://www.meteo.fr/vaac/eliens.html) runs the MOCAGE model.

Operational satellites primarily use infrared sensors for meteorological data because of the day and night capabilities. Ash can be detected through differences in the brightness temperature due to ash transmission changes between 10 and 12 mm channels (split-window technique). For this to be effective, light from underlying, higher temperature surfaces must pass through a semi-transparent ash cloud for detection at the satellite. Unfortunately fresh ash clouds during or immediately after the eruption are too dense to transmit IR light and must thin by fallout and dispersal by wind shear before they become semi-transparent.

Detection of ash clouds within 5 minutes or even within 12 hours is generally not possible with the IR split window technique. Thus, the current operational technology cannot routinely meet the requirement for detection of fresh ash clouds. Even when detected not all ash clouds are tracked after they have thinned. Water vapor and ice absorb at the same wavelengths and can completely mask the ash signal. High clouds below the ash may be near the same temperature as the ash resulting in no ash signal. In addition to missed detections of ash, other effects mimic the ash signal thus producing false alarms. The result is that the IR data require close analysis and interpretation by observers before it can be used for aviation warnings. For example, London VAAC uses the IR SEVIRI instrument on the geostationary MSG satellite, however, their automatic system currently detects only about two thirds of the eruptions.

Enhancement using NASA OMI research data

NASA research satellites have been used to detect volcanic eruption clouds for over 30 years. In fact the first observation of a volcanic sulfur dioxide cloud was made with backscattered solar UV data from the Total Ozone Mapping Spectrometer (TOMS) on the polar orbiting Nimbus 7 satellite in 1982. In addition ash clouds are also detectable by their light scattering properties in absorption-free channels. The current effort is focused on making this information available in near real-time (<3 hours) from new UV instruments for use by operational staff during volcanic events.

Sulfur dioxide is a unique component of magmatic eruptions that is easily detected at the UV wavelengths that are used to monitor ozone. Background levels of SO_2 are near zero and all other sources are orders of magnitude smaller than volcanic eruptions. Thus the appearance of a large SO_2 cloud immediately implies an eruption, and mapping instruments, like TOMS, can track this volcanic cloud globally until the SO_2 is converted to sulfate over about 30 days. TOMS instruments have now been replaced by new hyperspectral instruments, such as the Dutch/Finnish Ozone Monitoring

Instrument (OMI) on the EOS Aura platform. This instrument has the same daily globally contiguous mapping as TOMS, but smaller field of view and higher sensitivity allow better plume contouring and longer detection, that is essential for daily tracking of volcanic clouds. OMI was selected for this cooperative experiment with partners in NOAA and USGS.

Use of SO_2 as marker for ash clouds

SO_2 is not an immediate flight hazard to aircraft although long-term damage from the resultant sulfuric acid aerosol is possible. However, it has become apparent that the explosive eruptions that produce fine ash at aircraft cruise levels near the tropopause also contain SO_2, one of the gases that cause the explosive eruption. Thus, an explosive eruption ash cloud initially contains SO_2. The ease of detection of SO_2 without any false alarms makes this a very attractive marker for fresh ash clouds. Coarse ash grains fall out rapidly leaving only the finer grains to drift with the aging SO_2 cloud. The ratio of fine to coarse ash seems to vary with different eruption styles, and secondary processes, like electrostatic clustering, can produce rapid fallout. In addition, mixed eruptions, like phreomagmatic eruptions, produce low altitude ash clouds from each explosion with the altitude depending on the source. More work is required to characterize ash clouds from different eruptions.

Use of OMI Absorbing Aerosol Index to detect ash clouds

Ash clouds, as well as dust and smoke clouds have been long observed in the UV Absorbing Aerosol Index (AAI) from the TOMS instruments. This index compares the spectral distribution of light scattered by aerosols with the spectrum of Rayleigh scattering as a measure of aerosol optical depth. In contrast with the IR ash signal that depends on transmission through thin ash clouds, the UV AAI is immediately detectable from any ash cloud, thick or thin. Thus, fresh ash clouds can be detected immediately after an eruption. The combination of OMI data on SO_2, which also is immediately detectable, and AAI ash data provides a valuable dataset to determine the separation of ash and gas in volcanic clouds and to diagnose the character of the eruption.

Development of near real-time volcanic products

Evaluation of OMI standard products

The OMI Science Team developed standard algorithms to produce products for scientific use and archival. The OMSO2 Band Residual Difference (BRD) algorithm exploited wavelengths selected for maximum sensitivity to measure the smallest SO2 column amounts found in air pollution and volcanic degassing. For maximum speed and efficiency, it depended on radiance residuals at SO_2 band extremes computed by the operational OMTO3 total ozone retrieval algorithm. This utilized the OMTO3 soft calibration enhancements to reduce errors in background regions. We originally adopted this code for NRT processing at GSFC SIPS for delivery of Level 2 data to NOAA/NESDIS/OSDPD. Because of the BRD high SO_2 sensitivity, small sources, such as degassing volcanoes, could be monitored for non-eruptive and pre-eruptive volcanic activity. While not directly related to the drifting ash cloud problem, this new information was of great value to the USGS volcanologists, who are responsible for identifying volcanoes that are potentially capable of explosive eruptions. Prior to the OMI mission, this information could only be obtained by deploying hand operated instruments to each volcano. With OMI, all volcanoes around the world can be monitored on a daily basis. This is possible only because of the daily contiguous global coverage similar to TOMS, the option of picking optimum wavelengths from the OMI complete spectral coverage that was not available with TOMS, and is enhanced because the ground resolution is 8 times better than TOMS.

Development of new volcanic cloud algorithms

An eruption of Sierra Negra volcano in the Galapagos Islands in October 2005 showed that the standard OMSO2 algorithm produced very large errors, including negative SO_2 amounts, in the center of large SO_2 clouds. In addition, the AAI algorithm failed under the same conditions. The cause was determined to be a failure of the OMTO3 code due to the presence of SO_2 in large amounts. Consequently, we developed a second linear algorithm to correct the OMTO3 errors. This permitted valid SO_2 retrievals for amounts up to 500 times larger than background levels. In addition a new AAI algorithm was developed to fit the scattering spectral slope directly to avoid OMTO3 biases.

Several improvements were made to the operational system, including major noise improvements in OMI SO_2 data, resolution of background offset correction failure in OMI near real-time (NRT) data, and completion of the error analysis of the OMI Linear Fit (LF) algorithm.

A second artifact in the OMTO3 code had to be corrected before reliable SO_2 products could be produced. OMTO3 used a cloud height climatology developed for TOMS retrievals that made use of IR cloud top temperatures to infer heights. OMSO2 retrievals showed high SO_2 amounts over tropical clouds. These levels were too high to allow automated detection of volcanic eruption clouds. The problem was corrected by using effective cloud pressures determined using rotational Raman scattering filling in of Frauenhofer lines in the OMI spectral reflectance data. The radiative effective height of clouds at UV wavelengths was found to be much lower than the IR heights. Thus, OMTO3 corrections for tropospheric ozone in cloudy conditions were incorrect and the residuals at SO_2 wavelengths were wrong.

In the largest volcanic eruption clouds SO_2 amounts can be 5000 times greater than background levels. The retrieval errors were unknown in these conditions so a completely new Iterative Spectral Fitting (ISF) algorithm was developed. This code solves for all absorbers and scatterers simultaneously to provide self-consistent solutions. However, is too slow for NRT use but is used off line for special volcanic cases to evaluate retrieval errors, which were as large as a factor of two in the largest eruptions. In addition, the ISF algorithm was capable of determining the height of volcanic clouds if an additional iterative step is included. This new Extended ISF code is also used off-line for special cases.

Development of OMIPlot graphic analysis utility

SO_2 emissions detected in OMI Level 2 data vary over 5 orders of magnitude and special graphics tools are need to visualize the plumes and to analyze the properties. Using the TOMSPlot utility as a model, a new IDL OMIPlot utility was written to provide user-specified local or regional to global plots of SO_2, reflectivity, and aerosol index data, create L2 data subsets and postscript images, calculate total SO_2 mass within the plume, and various other tasks. In addition, a lite version was created for export to DSS users. An example of a data product from the May 2006 eruption of Soufriere Hills volcano on Montserrat, West Indies follows:

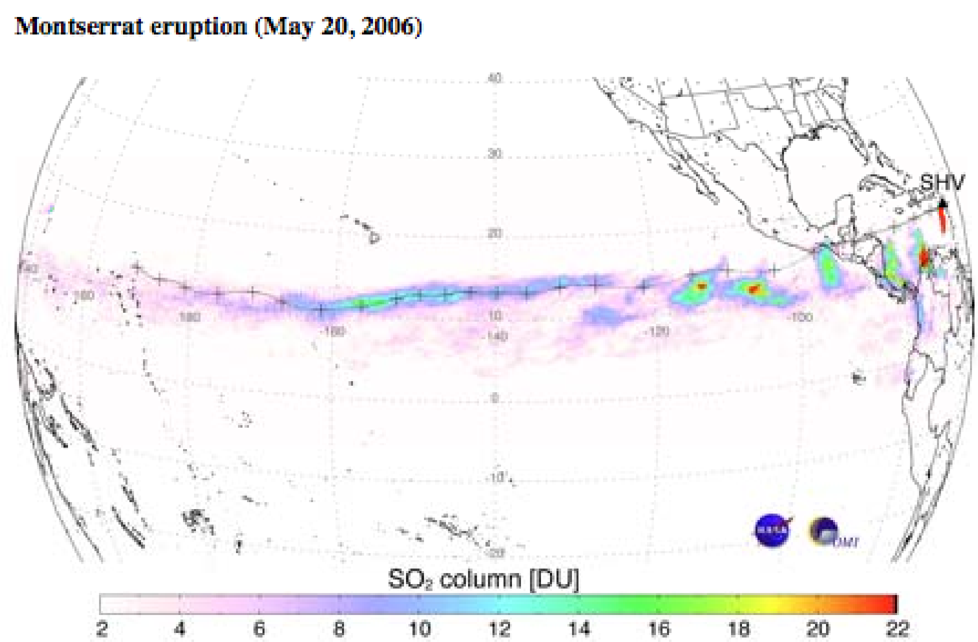

Requirements for Decision Support Services (DSS)

The DSS agencies, including the Volcanic Ash Advisory Centers (VAAC), the USGS Volcano Observatories and the NOAA NWS forecast offices, and airline dispatchers were consulted about the nature of the volcanic ash cloud data that would be useful. It was concluded that a web site was satisfactory for development purposes. The site would deliver image products in commonly used formats, as well as data subsets. This was implemented at the NESDIS/OSDPD offices.

It was later found that the Washington VAAC used only information available through N-AWIPS channels. An effort to place the OMI information in that form is in progress at the end of the current grant.

Near real-time data production

The OMI instrument was produced by a Dutch and Finnish collaboration and is flown on the US NASA Aura spacecraft. The Science Team is composed of US, Dutch, and Finnish scientists. By agreement the Level 1 and 2 data are produced at Goddard Space Flight Center in the SIPS. The Aura Project agreed that the Level 1b data remained the property of the Dutch and that NASA would not release the data to outside organizations. The reason was that the instrument calibration was evolving during the mission and only a single set of standard data products would be retained. This could only be guaranteed if the data remained within the Aura archival facility. Thus the NRT Level 2 OMSO2 processing was conducted at GSFC, rather than at NOAA. A unique NRT processing stream was developed and NOAA agreed to pull the data as it was produced.

The SIPS NRT processing was reliable, but the lack of 24 hour/7 day/week maintenance made it susceptible to outages in an operational system. There were problems on weekends when the SIPS computers failed because service could not be restored until personnel arrived on Monday mornings. This was upsetting at times when volcanic activity was being monitored closely. Thus, a completely operational system is a necessity for routine use by NOAA. This was in part alleviated when the GOME-2 instrument was launched on the European MetOp A operational satellite in 2006. The data are captured in the NOAA operational stream and thus are maintained at all times.

Operational detection of eruptions

Since the OMI activation in August 2004, approximately 45 volcanic eruptions from 26 volcanoes have been monitored in near real-time. An example of an unusual eruption that was disseminated to the tracked and global community is the eruption of a Red Sea volcano as shown below.

(Jebel al-Tair eruption)

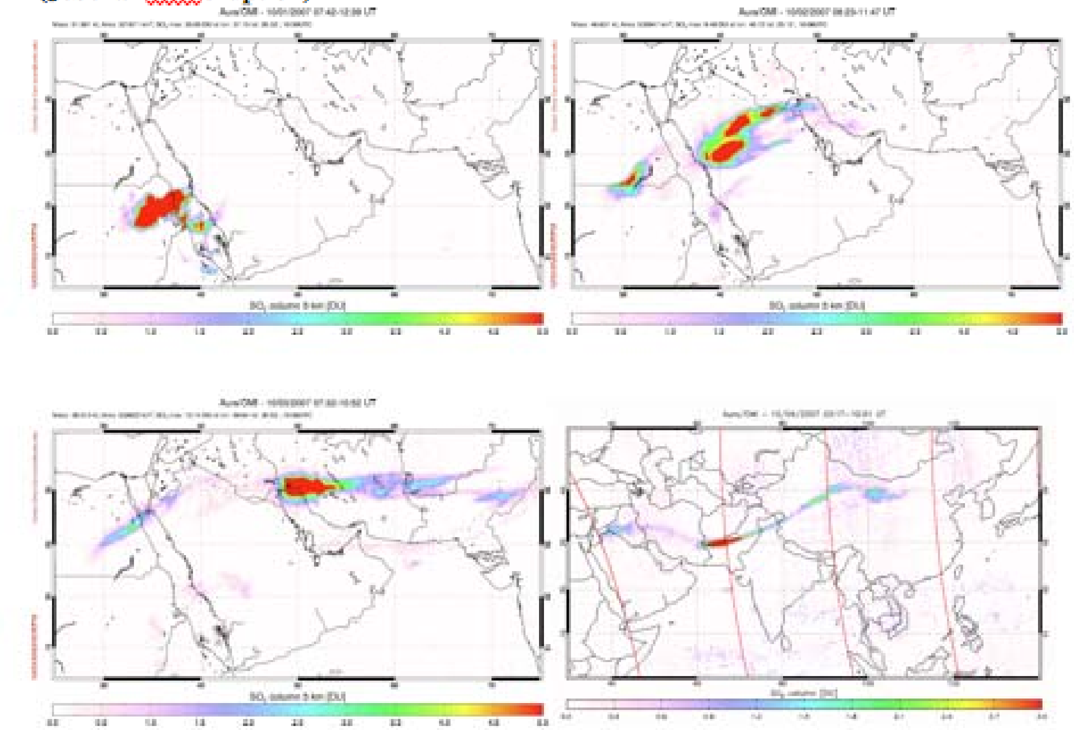

Figure 1 Jebel al Tair volcano in the Red Sea, thought to be extinct, erupted on September 30, 2007 and produced a sulfur dioxide cloud that was stretched by subtropical jet stream winds across southern Asia. The plume altitude, near the tropical tropopause at 17 km, measured in Calipso data, was above typical aircraft flight altitudes. This effusive eruption from a basaltic volcano produced only a small amount of ash that fell out near the island.

Monitoring of degassing from active volcanoes.

Hundreds of volcanoes are now being monitored for degassing by the USGS and international organizations using OMI daily data. Several volcanic crises merited attention. One example is shown below in which large population centers were threatened. Volcanologists are usually called in by local officials to help decide whether evacuation is necessary. They normally depend on trends in seismic data and local measurements of sulfur dioxide emissions. With OMI data they can now get daily views of the SO2 emissions and, in addition, see what other volcanoes in the same region are doing.

Merapi crisis (April – June 2006)

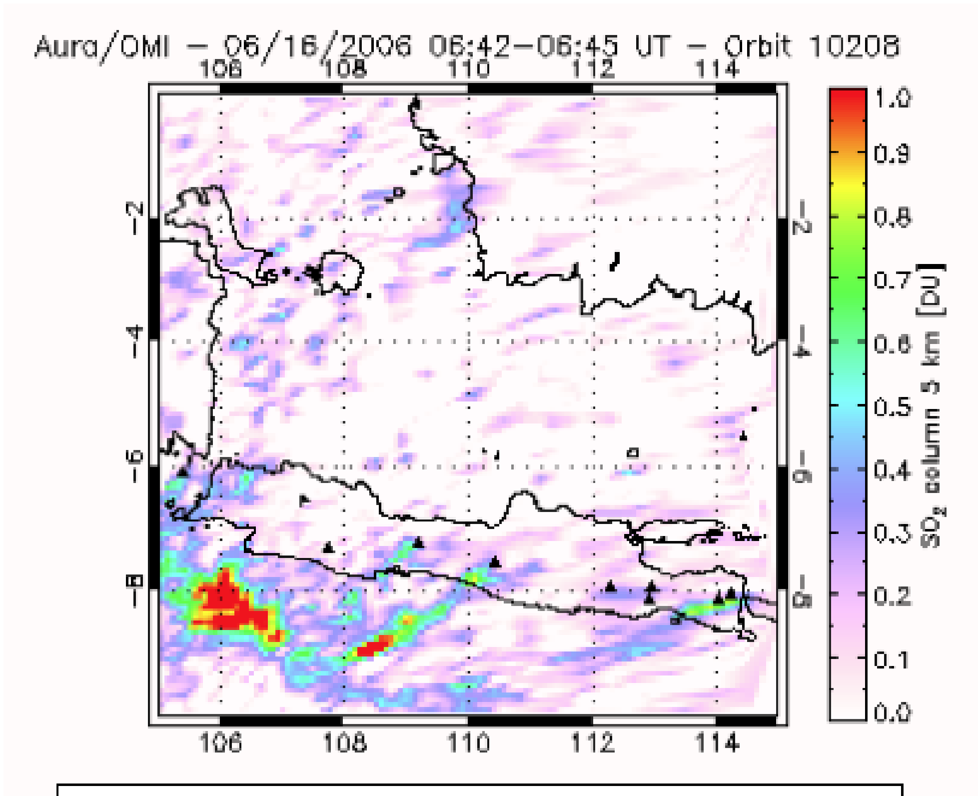

Figure 2. OMI images on June 16, 2006 of outgassing from three volcanoes on Java shown by the trails of sulfur dioxide drifting southwest from volcanoes. Merapi (the central volcano) threatened large population centers but released internal pressures by outgassing.

In 2006, Merapi volcano in central Java was threatening to erupt based on seismic data and rockfalls from dome building. NRT OMI data were available to follow the daily changes in degassing. It was found that other volcanoes on Java more active in SO_2 emissions than Merapi. This provided evidence for volcanologists that Merapi was not an immediate hazard. In fact, the activity abated after a few months.

Several volcanoes in Ecuador and Columbia became active in 2007 – 2009. They include Tungurahua, Huila, and Reventador. We provided OMI images and daily emission tonnages to the local volcanologists for their assessment of eruption probability.

Data availability on the web

Data produced in NRT are available from the NOAA web sites:

http://satepsanone.nesdis.noaa.gov/pub/OMI/OMISO2/index.html

and

http://satepsanone.nesdis.noaa.gov/pub/GOME/GOMESO2/index.html

Archived production volcanic images and data from both OMI and TOMS are available at the UMBC web site:

http://so2.umbc.edu

OMI instrument and standard SO_2 algorithms

The NASA EOS Aura platform, launched on July 15, 2004, carries the Ozone Monitoring Instrument (OMI), a hyperspectral UV/Visible spectrometer with a 2600 km swath for daily, global contiguous mapping that was provided by the Netherlands Agency for Aerospace Programs (NIVR) in collaboration with the Finnish Meteorological Institute (FMI) to the NASA EOS Aura mission for continued monitoring of ozone and other trace gases . KNMI (Royal Netherlands Meteorological Institute) is the Principal Investigator institute. Reflected sunlight in a fan-shaped narrow field of view is dispersed by a spectrometer and imaged in spatial – spectral dimensions on two-dimensional Charge Coupled Device (CCD) detectors, one for UV and one for visible bands. We use data from the 310–365 nm UV-2 band of OMI with spectral resolution of ~0.45 nm. Data are collected from the pushbroom swath in 2-second intervals corresponding to 13 km along-track resolution. Pixels are binned in 60 cross-track positions to provide a nadir resolution of 24 km. A solar calibration is taken at the northern terminator.

Starting in 2006 we have produced data with the fast technique termed the Band Residual Difference (BRD) algorithm that utilizes four wavelengths that are positioned at SO_2 band extrema between 310.8 nm and 314.4 nm [Krotkov et al 2006]. Being less computationally demanding than a spectral fitting algorithm, the BRD method is also faster and applicable to generation of OMI SO_2 data in a near-real time operational scenario. The BRD algorithm was used to produce initial Level 2 SO_2 data until it was replaced by more robust linear fit algorithm [Yang et al 2007]

Algorithm Description

We use two different algorithms to produce SO_2 column data from OMI. The Planetary Boundary Layer (PBL) columns are produced using the Band Residual Difference (BRD) algorithm [Krotkov et al 2006], while lower troposphere (TRL), middle troposphere (TRM) and lower stratosphere (STL) columns are produced with the Linear Fit (LF) algorithm [Yang et al 2007]. Both algorithms use a recently modified version (Version 8.5) of TOMS total ozone algorithm (OMTO3) [Bhartia and Wellemeyer 2002] as a linearization step to derive an initial estimate of total ozone assuming zero SO_2. The residuals at 10 selected wavelengths are then calculated as the difference between the measured and computed N-values ($N=-100*log_{10}(I/F)$, I is Earth radiance and F is solar irradiance) using a vector forward model radiative transfer code that accounts for multiple Rayleigh scattering, ozone absorption, Ring effect, and surface reflectivity, but assumes no aerosols. Cloudy scenes are treated as mixture of two opaque Lamberian surfaces, one at the terrain pressure and the other at Radiative Cloud Pressure (RCP) derived using OMI-measured Rotational Raman scattering at around 350 nm. In the presence of SO_2, the residuals contain spectral structures that correlate with the SO_2 absorption cross-section. The residuals also have contributions from other errors sources that have not yet been identified. To reduce this interference, a median residual for a sliding group of SO_2-free and cloud-free pixels (OMTO3 radiative cloud fraction < 0.15) covering $\pm 15^o$ latitude along the orbit track is subtracted for each spectral band and cross-track position [Yang et al 2007].

Both the BRD and LF algorithms use the corrected residuals as their inputs to derive SO_2 column amount. The BRD algorithm works best in presence of anthropogenically produced SO_2, since they do not affect the total ozone derived by the OMTO3 algorithm. This algorithm uses differential residuals at the three wavelength pairs with the largest differential SO_2 cross-sections to maximize sensitivity to anthropogenic emissions in the PBL. Each pair residual is converted to SO_2 slant column density (*SCD*) using differential SO_2 cross-sections data at constant temperature (275 K) [Bogumil et al 2003]. The *SCDs* of the three pairs are averaged and the average *SCD* is converted to the total SO_2 vertical column density (VCD) using a constant air-mass factor (*AMF*) of 0.36. This *AMF* was estimated for cloud- and aerosol-free conditions, using a solar zenith angle of 30^o, nadir viewing direction, a surface albedo of 0.05, a surface pressure of 1013.3hPa, a 325 DU mid-latitude ozone profile and a typical measured summer SO_2 vertical profile over the Eastern US. Krotkov et al [2008] provide an estimate of how the *AMFs* vary with observing conditions**.**

SO_2 produced by volcanic eruptions can produce large errors in OMTO3 derived total ozone and can make the retrieval highly non-linear. The linear Fit (LF) algorithm was developed to handle such cases. The LF algorithm minimizes different subsets of residuals by simultaneously adjusting total SO_2, ozone and scattering using a quadratic polynomial in the spectral fit. The subsets are determined by the process of dropping the shortest wavelength bands one at a time until the 322nm band is reached. The largest SO_2 retrieval is reported as the final estimate. The assumed gaseous vertical profiles correspond to the standard OMTO3 ozone profiles. The SO_2 weighting functions are approximated using OMTO3 layer Efficiency factors in Umkehr layers 0, 1 and 3, for ColumnAmountSO2_TRL, ColumnAmountSO2_TRM, and ColumnAmountSO2_STL data. Correspondingly. treatment of aerosols and clouds is the same as in the OMTO3 algorithm.

NRT OMI data production

Level 2 OMSO2 production - NASA GSFC/SIPS

The OMI Science Investigator-led Processing Systems (SIPS) is a data processing system based at NASA's Goddard Space Flight Center in Greenbelt, Maryland. In addition to performing the operational processing for OMI, it also has a near-real-time (NRT) processing component. For NRT, latency is of key concern, so the OMI SIPS receives Rate Buffered Data (RBD) directly from the EOS Data and Operations System (EDOS) with minimal processing. The RBD process omits things like time ordering and duplicate packet removal, so the data aren't as 'clean' as the operational processing stream, but this allows the data to be processed as quickly as possible. The OMI SIPS applies the Level 1B processing using the Ground Data Processing System (GDPS) supplied by the Royal Dutch Meteorological Institute (KNMI). For the NRT processing, some of the more time consuming processing steps are disabled, including: spectral calibration, solar stray light corrections and some dark current corrections. The OMI SIPS then applies several Level 2 processing algorithms to the Level 1B data, including the OMSO2 retrieval. The resulting products are then pushed onto a staging site where they are available for a pull by operational customers of the products. In order to improve system availability, the OMI SIPS is currently deploying a redundant backup system that will process all NRT data in parallel with the primary system. To reduce the single points of failure even further, EDOS is deploying a backup instance of their system as well.

The OMSO2 product is written as an HDF-EOS5 swath file. Data files are available from Goddard Earth sciences Data and Information Services Center (GES DISC) web site. A file, also called a granule, contains SO_2 and associated information retrieved from each OMI pixel from the sun-lit portion of an Aura orbit. The data are ordered in time sequence. The information provided on these files includes: latitude, longitude, solar zenith angle, OMTO3 reflectivity (LER) and independent estimates of the SO_2 vertical columns, as a well as a number of ancillary parameters that provide information to assess data quality. Four values of SO_2 column amounts are provided corresponding to four assumed vertical profiles. Independent information is needed to decide which value is most applicable. For a complete list of the parameters, please read the OMSO2 file specification: (http://so2.umbc.edu/omi/ click on Documentation and OMSO2.fs). These files are pulled by the NOAA partners as they are produced.

Processing and distribution - NOAA/NESDIS

The NOAA/NESDIS data processing code has been developed to retrieve the OMI data products and generate images to be displayed on a public web server. The data are received by NOAA through an automated ftp script which checks to see when a new

OMI orbital file has been processed and staged on a NASA server. These files are received as a Hierarchical Data Format (HDF) file and temporarily stored in on a NOAA server where it will be processed. The primary set of processing code, used to decode the data and process the OMI orbit images, resides on this server and routinely checks to see if a new orbital file has been received. When a new orbit is found, the data file is decoded and loaded into McIDAS. The mapping tools offered by McIDAS allow for the quick generation of maps displaying the various OMI products. Using these McIDAS tools, global composite SO2 images and regional single-orbit images are generated. A series of html pages to display these images are also generated. Upon completion, the image and html files are transferred to a web-server where the OMI data are made available to the public.

McIDAS

McIDAS is the main environment where the OMI data are processed and analyzed in NOAA. In existence since 1973, McIDAS (Man computer Interactive Data Access System) is a suite of sophisticated software packages that perform a wide variety of functions with satellite imagery, observational reports, numerical forecasts, and other geophysical data. Those functions include displaying, analyzing, interpreting, acquiring and managing the data.

Data evaluation tools

OMIPlot utility

A data evaluation tool called OMIPlot was developed to aid in the analysis of the OMI data products. OMIPlot is a software package written in the Interactive Data Language (IDL). The main function of OMIPlot is to enable the user with the ability to map OMI data onto many different mapping projections. However, the software package also allows the user to compute statistics on the OMI datasets and query information on individual measurements.

Features

OMIplot allows users to either interactively generate and analyze or auto-generate images from OMI data products. In both cases the user can decide to work with a single orbit, a full day of OMI data, or averages of multiple days.

Mapping, projections

IDL offers users access to many predefined mapping projection routines, many of which were incorporated in OMIPlot. The following is a list of the current mapping projections supported by OMIPlot:

Orthographic
South Polar Stereographic
North Polar Stereographic
Geosynchronous satellite
Stereographic
Azimuthal equidistant
Mercator
Mollweide
Hammer-Aitoff
Sinusoidal
Cylindrical Equidistant

For each of these projections, the user can easily adjust the mapping scale (or mapping limits). This is important since the scaling limitations for the listed projections are not necessarily the same. As such, individual scaling routines were written for many of the different projections.

Data Filtering

Several filters were developed to allow different subsets of the OMI Data to be displayed. These filters allow users to subset data based on X-track position, solar zenith angle, cloud-top pressure, and SO_2 Quality flag.

Gridded or FOV Display

Two data plotting methods were developed to display OMI data: Gridded Display and Field-of-View (FOV) display. The gridded display option interpolates the inputted OMI data onto an equi-spaced lat/lon grid, where the grid size can be defined by the user. This is especially useful when loading a full day of OMI data. The FOV display option computes the field-of-view for each measurement and renders a representation of each measurement's "footprint" projected on the predefined map projection.

Tonnage

For each processed image, regional SO_2 tonnage calculations are preformed. By changing the mapping scale, one changes the region over which the tonnage is computed. This is particularly advantageous when attempting to compute SO_2 mass calculations for individual SO_2 clouds. An option to specify the latitude – longitude corners of a cloud box, as well as a background box, is available for detailed analysis.

PS Output

The OMIPlot software was written to produce images in Post-Script (PS) format. When outputting a displayed image to a PS file, both orbital and statistical information about the data used to produce the image is added to the PS file. The resulting images are rendered at publication quality.

Data extraction: ASCII, IDL, and KML

The data used to construct an image can be extracted into three formats: a text (ASCII) file, an IDL save file, and as a KML file. For most users, text output data is a standard method of data storage. For IDL users, storing data in an IDL save is convenient as it can be easily loaded into IDL "as is". The third output format is a rather new data format that is designed to be compatible with the Google Earth ™ mapping software. Google Earth ™ has recently become a popular tool used to create high-resolution maps from satellite imagery.

Standard OMI algorithm evaluation

Background offset correction

Background amounts of SO_2 of less than 0.1 DU are expected to be below OMI detection limits and instrument radiometric calibration uncertainties. The latter can be removed by forcing the OMTO3 residuals to be zero in background areas. This stabilizes the data as long as real SO_2 is not included in the background areas. This technique appears to work well except for high solar zenith angles. However, the background-corrected offsets still are subject to biases at high latitudes that are correlated with total ozone variations.

Sierra Negra artifacts; failure of the OMTO3 algorithm with high SO_2

The eruption of the Galapagos volcano, Sierra Negra, in 2005 produced an initial high altitude plume followed by days of outpouring of SO_2 in the typical pattern of effusive eruptions. However the spatial pattern of SO_2 was unexpected in that a hole appeared in the middle of the plume with even negative values. The problem was traced to the OMTO3 algorithm which was designed to assume SO_2 was ozone. When real SO_2 appeared the residuals computed at SO_2 wavelengths were completely erroneous because the total ozone was wrong. To correct this situation a new Linear Fit (LF) algorithm was developed that sequentially computed SO_2 using combinations of the longer wavelengths, finding the largest value, and using that to correct the ozone. This algorithm was incorporated in the OMSO2 module and has reliably delivered useful results in all except the largest SO_2 clouds.

Cumulus cloud artifacts and failure of the IR cloud height climatology

False SO_2 blips were found in the tropics in association with convective clouds. An investigation showed that they were due to the use of inappropriate cloud heights by the OMTO3 algorithm. Historically, cloud heights from IR cloud top temperature data had been used to correct for tropospheric ozone in the total column retrieval. With OMI's hyperspectral data a UV cloud pressure can be derived from either O2 – O2 absorption or by backfilling of Frauenhofer solar lines from Rotational Raman scattering. Both techniques found that the effective height of clouds was lower than the cloud top height sensed at IR wavelengths. When the Effective UV cloud pressure values were used the SO_2 cloud artifacts were removed. This change served to improve the total ozone database as well.

Ash algorithm development

An Aerosol Index (AI) was developed in TOMS data analysis as a flag for dust and smoke clouds which affect the total ozone retrievals. The look-up tables used to infer total ozone were created using a Rayleigh scattering radiative transfer model. Aerosols change the spectral distribution of scattered light so the tables produce retrieval errors under dusty conditions. AI is just a relative indicator of deviation from Rayleigh scattering that is useful for finding things like Saharan dust and smoke from forest fires. Volcanic ash scatters light similarly to dust and the AI was found to be a reliable locator of ash clouds. Unfortunately, the AI is usually wrong if SO2 is present to corrupt the ozone retrievals. Particularly in the large ash clouds from Kasatochi the AI values were even negative in the middle of the plume.

With OMI data it is possible to fit the non-absorbing spectral slope using many wavelengths, even those affected by ozone absorption but after correction for the sO2 induced errors. The spectral slope is a robust measure of ash scattering but must be scaled by a factor of 2700 to get a value similar to the conventional values. This is incorporated in current NRT production of ash cloud data.

NOAA data distribution

Polling of DSS needs

Infusion of SO_2 data from NASA satellites into volcanic hazard Decision Support Systems (DSS's) operated by the National Oceanic and Atmospheric Administration (NOAA) and the US Geological Survey (USGS), which provide aviation alerts to the Federal Aviation Administration (FAA), will reduce false alarms and permit more robust detection and tracking of volcanic clouds, the development of an eruption alarm system, and potential recognition of pre-eruptive.

Volcanic Degassing: HTML Output

A website[1] was developed to allow users of the data to easily and quickly find and interoperate processed OMI SO_2, Reflectivity, and AI products. The products are display through two different methods: composite maps and single orbits. The composite maps display the last 24 hours of SO_2 data and are generated for three regions: the Tropics, Northern Hemisphere, and Southern Hemisphere. An example of the area covered by each of these regions is shown below.

Tropics

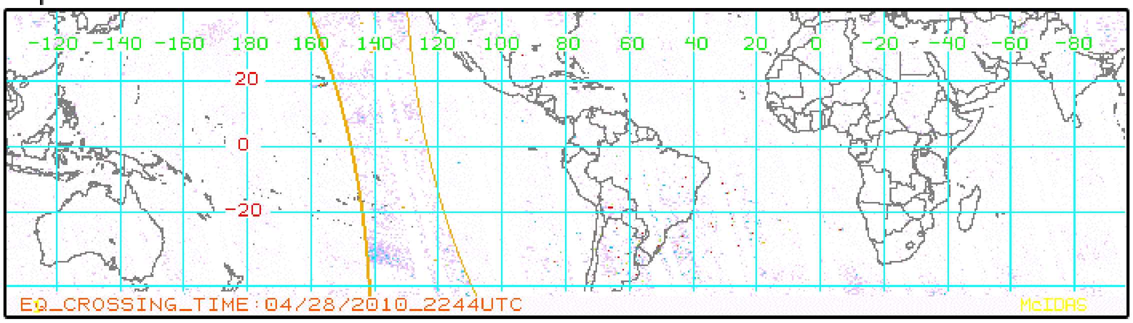

Northern Hemisphere

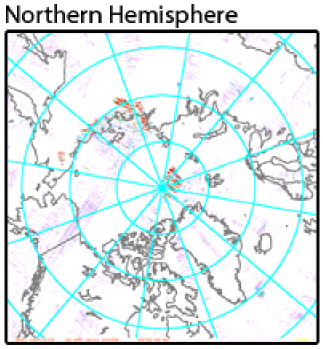

Southern Hemisphere

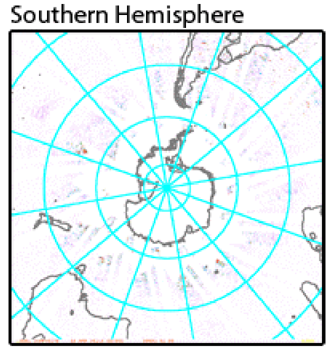

The data for these three regions can either be viewed interactively or downloaded. Through the usage of a Java applet, the user can zoom into each of these composite areas to better resolve features in the data. However, the data for each for these displays can be downloaded in the following formats: GIF, NetCDF, GeoTIFF, and McIDAS. An archive of composites for the previous 17 days are also made available in the previously mentioned formats. The non-composite, or single orbit, displays were developed to display the activity within specific regions of volcanic activity.

The OMI Near-Real-Time products website can currently found at: http://satepsanone.nesdis.noaa.gov/pub/OMI/OMISO2/index.html

Development of volcanic region subsets

There are currently 30 regions designed to show individual OMI orbits, a full list of these regions can be found at the end of this section. An example of the interface for these subset regions is shown below:

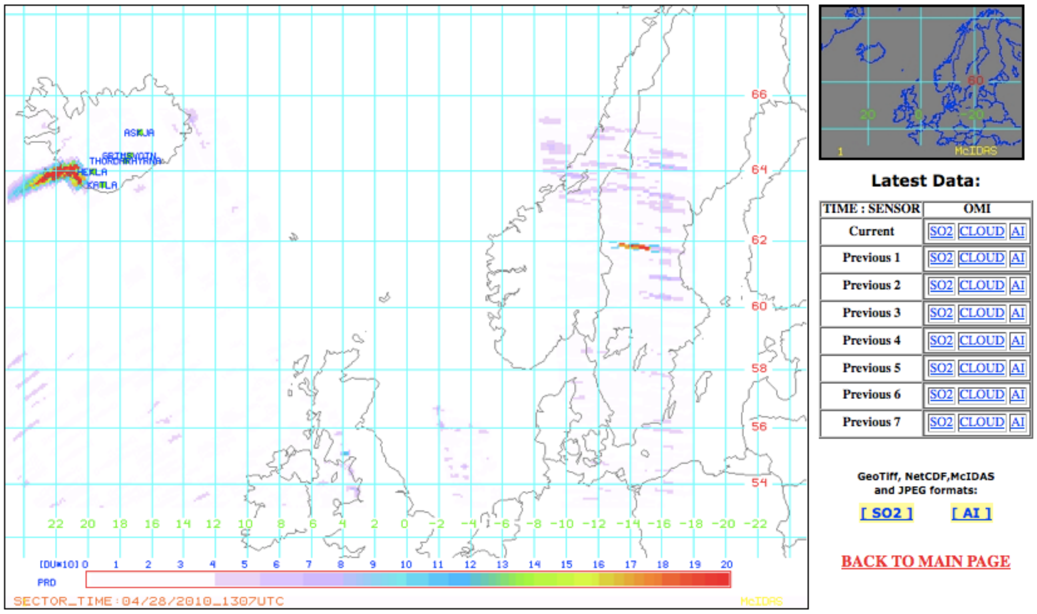

For each of these regions, the most current orbital overpass is displayed. The user also has to option of viewing the past seven orbital overpasses for this region. For each orbit, the user can view the SO_2, AI, and Reflectivity products. Like the composite images, the user can download the data from these orbits in GIF, NetCDF, GeoTIFF, and McIdas formats. URLs to a 17-day archive of the SO_2 and AI products are found on each region subset page.

List of volcanic region subsets:

Alaska, USA
Aleutian Islands, Alaska, USA
Anatahan, Mariana Islands
Cascade
Central America
Comoro Islands
Eastern China
Ecuador
Etna, Sicily, Italy
Galapagos Islands, Ecuador
Hawaii, USA
Iceland
Japan
Java, Indonesia
Kamchatka, Russia
Mexico
Montserrat, West Indies
New Zealand
Northern Chile

North Western Europe
Nyiragongo, DR Congo
Peru
Philippines
Papua New Guinea
Red Sea
Reunion Island
Southern Chile
Sulawesi Sangihe, Indonesia
Tanzania
Vanuatu, South Pacific

Selection of McIdas for product generation

A primary systems component of the W-VAAC is McIDAS, a sophisticated, video-interactive set of tools for manipulating satellite imagery, conventional meteorological observations, and other environmental information. McIDAS workstations, maintained by local NESDIS staff, are augmented by additional N-AWIPS (National Center Advanced Weather Interactive Processing System) workstations provided by and maintained by NWS/NCEP as part of the collaborative VAAC effort. The N-AWIPS workstations, also a primary DST at the AVAAC, are especially useful for display and analysis of weather data in conjunction with the output of several NWS forecast models.

Eruption alert generation

A system to detect the presence of large SO_2 clouds was developed to create an eruption alert system based on the OMI SO_2 product. After the images are processed through McIDAS, a set of codes search through the orbit for the presence of highly concentration of SO_2. If found, an image is produced showing the region where the SO_2 cloud was detected. An html page displaying this image is then generated and an automated e-mail is sent out with the URL of the html page. An example e-mail and html page generated from this alert system is shown below:

Subject: Alert: Potential Volcano Activity Detected - NOAA NRT System
From: oper@localhost.localdomain
Date: 6/15/2009 10:47 PM
To: gilberto.vicente@noaa.gov

```
Message from the NOAA OMI SO2 experimental automated alarm system
Anomalous SO2 concentration detected in the most recent OMI data
Check http://satepsanone.nesdis.noaa.gov/pub/OMI/OMISO2/Alert/alert.html for more details.
```

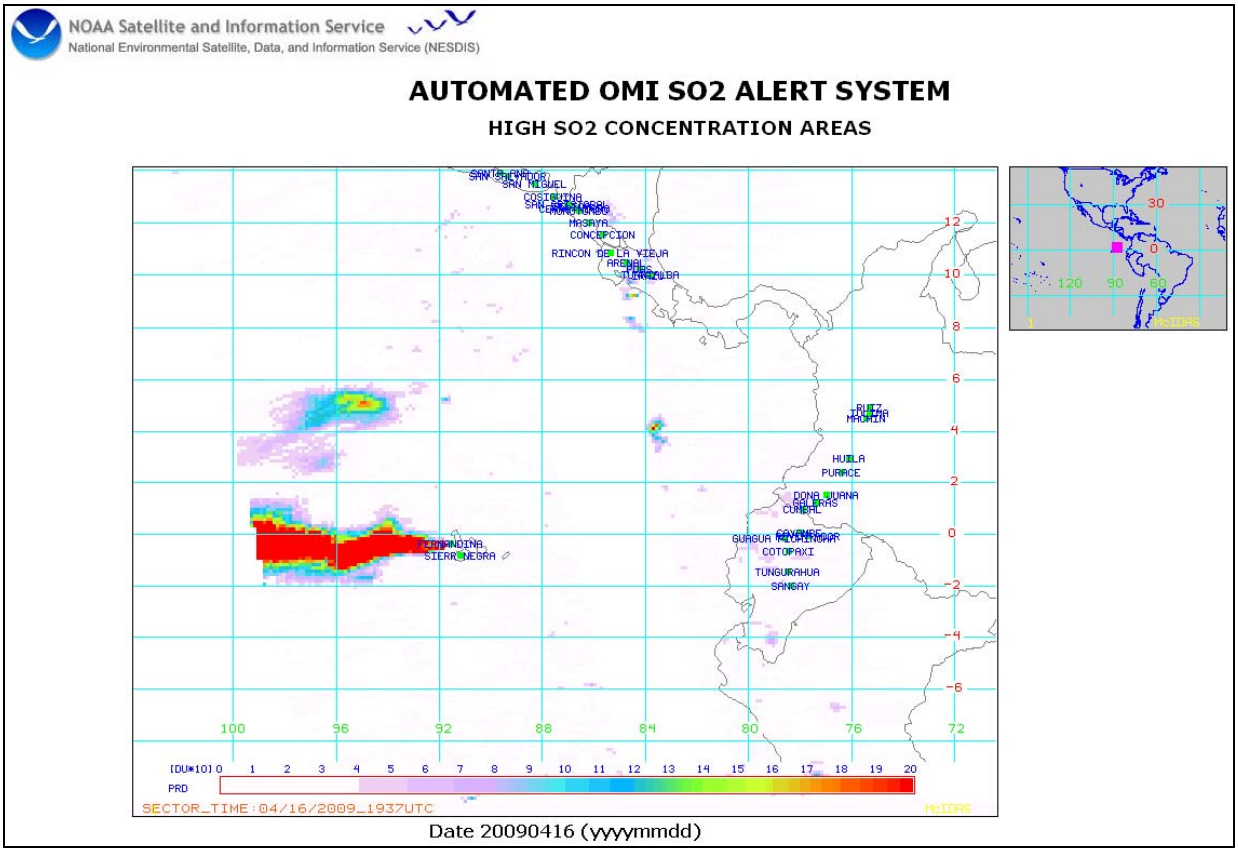

Examples of eruptions tracked

The system was used to track several volcanic eruptions during the first year of operation, including Tungurahua (Ecuador), Kilauea (Hawaii), Anatahan (Mariana Islands), and Etna (Sicily). The OMI-AIRS system detected SO_2 emissions following a small volcanic eruption near Manda Hararo, Afar, Ethiopia in August 2007; this event was featured on NASA's Earth Observatory (http://earthobservatory.nasa.gov/NaturalHazards/natural_hazards_v2.php3?img_id=14473).

Two significant volcanic events were also monitored. Based on an AIRS SO_2 alert received on September 30, 2007, the staff of the Washington Volcanic Ash Advisory Centers (VAAC) notified the Toulouse VAAC of volcanic activity in the Red Sea area near Yemen. Toulouse VAAC personnel had not realized an eruption had occurred at Jabal al-Tair, and as a result of the notification sent out an advisory to the aviation community shortly thereafter. The eruption was tracked in near real-time with OMI data for nearly 2 weeks (see figure in Summary section). The second significant volcanic event occurred on January 1, 2008, when the Llaima volcano in Chile erupted for about 12 hours, producing an 1100 km long plume that drifted over Argentina. The plume continued drifting eastward until conversion to sulfate four days later over the Atlantic Ocean (Figure 2). This event was detected by both OMI and AIRS.

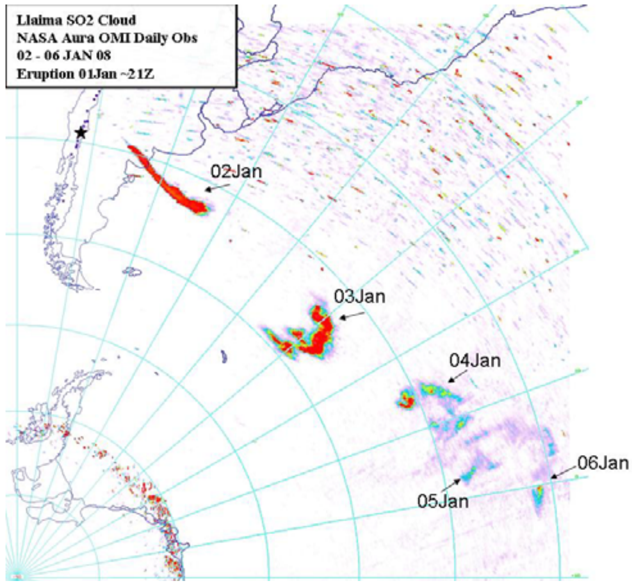

Llaima erupted on the evening of Jan 1. According to the Buenos Aires VAAC, the resulting ash cloud reached an altitude of 12.5 km (41,000 ft). On Jan 4, the volcanic SO_2 cloud drifted over Tristan da Cunha in the South Atlantic Ocean.

Later in 2008, two major north Pacific volcanoes seriously affected air traffic. On July 12, Okmok volcano in the western Aleutian Islands erupted to form an ash and SO_2 plume that drifted east toward the Canadian west coast. The ash fell out in two days but the SO_2 plume continued to drift east and south, producing a streamer that extended completely across North America. Fortunately, it drifted across Pullman WA, where the SO_2 amounts were validated by Dr. George Mount, using a research grade spectrometer.

One month later, a second Aleutian volcano, Kasatochi, exploded to produce 1.5

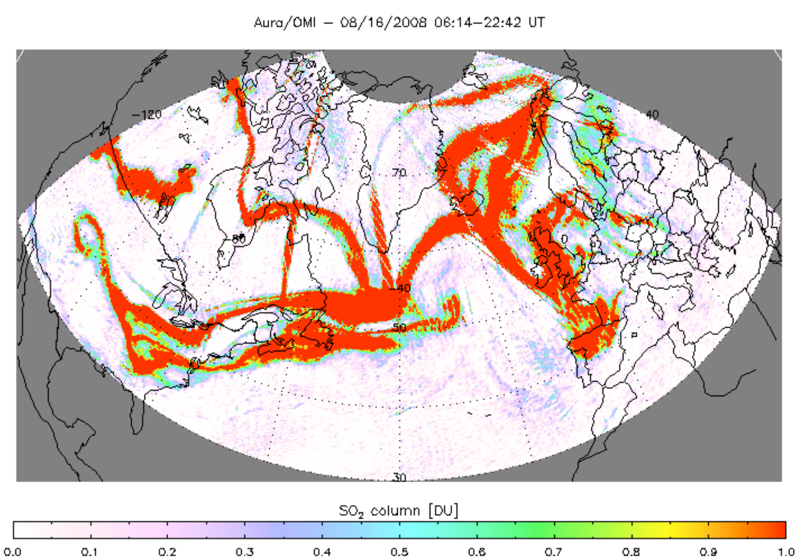

Tg of SO_2; the largest eruption since Mt Pinatubo in 1991. The ash cloud drifted with the SO_2 across the Gulf of Alaska before it fell out. The SO_2 cloud, however, was split into streamers that extended in a complex pattern all the way to Europe. The affect on air traffic was dramatic as the airlines learned how to deal with SO_2 clouds and the uncertainty of the ash concentrations.

In 2009 significant eruptions included Chaiten and Llaima, Chile; Fernandina, Galapagos; Redoubt, Alaska, which seriously affected air traffice through Anchorage; and Sarychev, Kurile Islands, another major source of interference with trans-Pacific air traffic. Kilauea, Hawaii began an extended period of degassing that continues in 2010 and Huila, Columbia showed extensive degassing.

Evaluation of volcanic ash cloud detection with OMI data

The premise of this investigation is that SO_2 is a reliable proxy for high altitude ash clouds. After examining about 45 eruptions with clouds persisting for at least 2 days we found that the relation between SO_2 and ash in volcanic plumes is complicated due to the different eruption processes and styles. We have observed eruptions where the ash followed different trajectories than SO_2, some where very little ash was produced, others where much ash was produced but little SO_2, and a number where the ash and SO_2 clouds were nearly identical until the ash disappeared by gravitational settling.

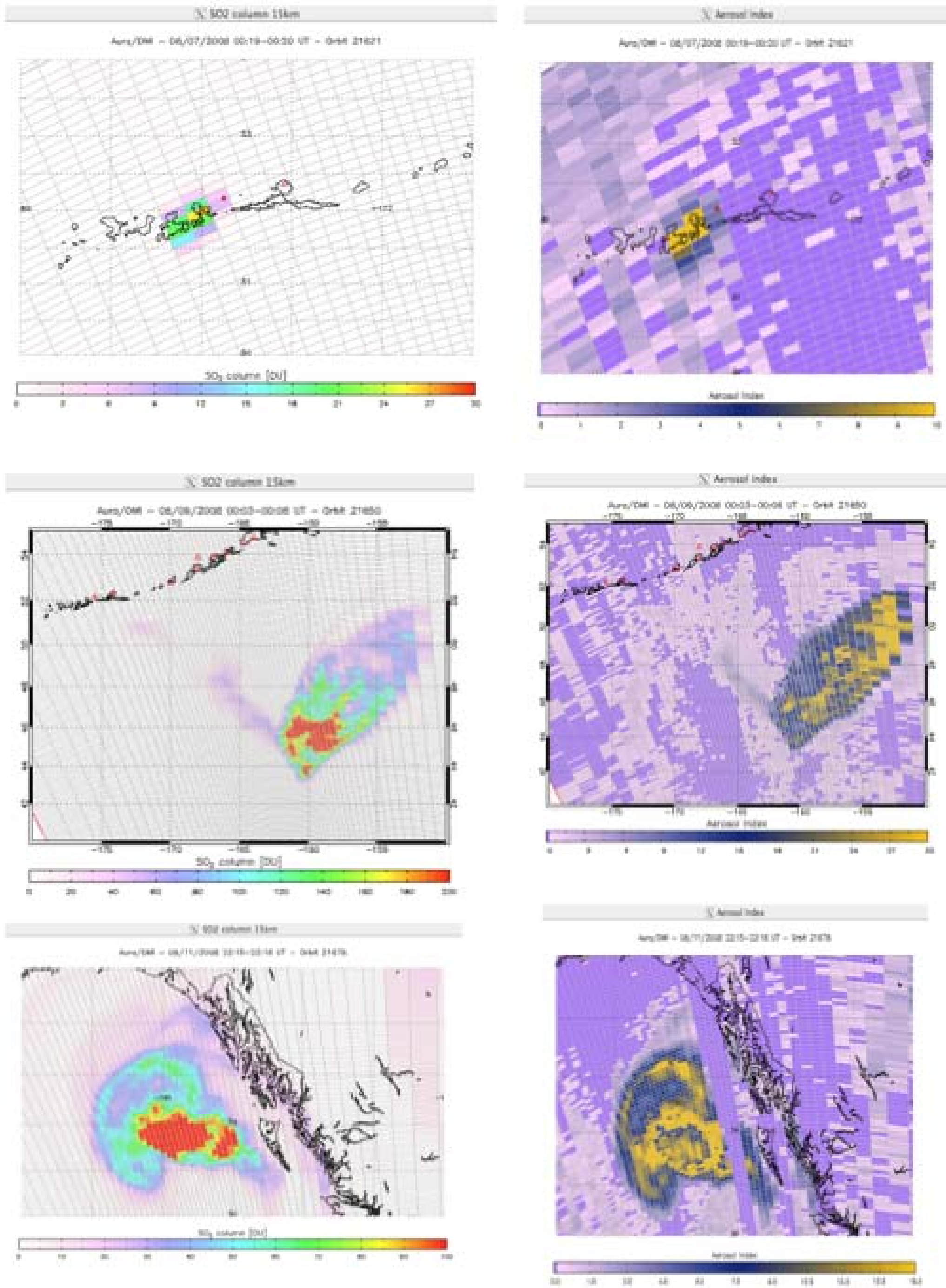

Coincidence between Kasatochi SO_2 (left) and AI ash (right) clouds over first 3 days after eruption on August 8, 2008.

This project is focused on the eruptions that produce hazards to aircraft at cruising altitudes near or above the tropopause. Ash at these altitudes is most commonly produced by explosive magmatic eruptions. We have a number of these eruptions to evaluate the ash – SO_2 relations. An eruption of Kasatochi volcano on the Aleutian Islands in August 2008 shows the close correspondence in the Figure above. The SO_2 and ash are detected within two hours of the eruption at 22:01 on August 7 and remain in the same cloud until August 12 when the ash disappears due to gravitational settling. An earlier eruption of Okmok on July 12 2008, also in the Aleutians, shows the same relationship although the circulation produced only a long streamer across North America. Other Northern Pacific eruptions over the past 20 years also produced the fine ash that only settles out after 3 – 4 days. Thus, we conclude that the OMI data provide a robust marker for ash clouds for explosive magmatic eruptions.

Early OMI detection of ash and SO_2

A second virtue of the OMI UV retrievals of ash is that the plume does not have to be transparent for detection. GOES split window ash retrievals did not detect the Kasatochi cloud until the next day because of water vapor screening of the earlier plume. Once IR detection was possible the UV and IR clouds were in exactly the same positions. The Okmok ash plume was never detected with the split window technique.

The reason for earlier detection by OMI is because it uses the scattering properties of the ash rather than the transmission, and other atmospheric constituents do not interfere with the scattering properties. Thus, a satellite monitoring system capable of detection of eruptions within 5 minute will have to rely on a UV technique rather than an IR method.

GOME-2 data added to the OMI coverage

In 2006, ESA launched the GOME-2 instrument in a morning orbit on the MetOp-A operational meteorological satellite in collaboration with the US NOAA polar satellite program. The instrument is a hyperspectral, cross-track scanning spectrometer with moderate ground resolution (40 x 80 km) maintained across the swath, and with almost daily contiguous global coverage. As part of the collaboration, NOAA receives all of the GOME-2 data in NRT. NOAA ORA has a research program that has developed the software to produce total ozone data.

In 2008, OMI an object below the spacecraft developed a partial obscuration in the earth field of view that affected coverage just right of the nadir. This obscuration was progressive and grew over the next year to about one-third of the swath. This has a profound affect on OMI daily coverage as well as on contiguous plume coverage. To mitigate this loss, we conferred with Dr. Lawrence Flynn of ORA and found that our OMSO2 code was compatible with the GOME-2 total ozone code (a derivative of the OMTO3 code). UMBC developed interface code and delivered a new GOMSO2 module to NOAA for NRT processing. This fully operational system is a clear advantage for volcanic hazard monitoring.

NOAA/OSDPD developed a GOME-2 website to run in parallel with the OMI website and production was initiated in 2009. This provided complementary data with morning coverage from GOME-2 and afternoon coverage from OMI.

In the GOME-2 evaluation we found significant differences from the OMI SO_2 retrievals in volcanic plumes as well as in background noise. The noise limits the smallest plume that can be measured. We found that the GOME-2 noise was more than

	Nimbus 7 TOMS	EOS Aura OMI	MetOp GOME-2
Nadir footprint (km) Scenes / scan	50 x 50 35	13 x 24 60	80 x 40 fixed footprint 24
Spectral resolution (nm)	1.1	0.45	0.26 – 0.28
Bands Wavelength span, nm	6 discrete bands 312.5 - 380	UV –2 310 – 365	Ch – 2: 311 - 403
SO_2 retrieval noise, 1σ (DU) for a cloud at 15 km	5	0.15	0.36
SO_2 detection limit (tons) 5 adjacent pixels > 5σ)	7000	26	650

twice the OMI noise under optimum viewing conditions and increased more rapidly as the solar zenith angle increased. The reason was found to be instrumental because the radiometric signal-to-noise ratio degraded very rapidly for wavelengths shorter than 320 nm where SO_2 has the best spectral properties for discrimination from ozone.

A second difference came from the inferior ground resolution of GOME-2 at nadir conditions. With a ten-fold larger footprint and the increased retrieval noise the detection limit of GOME-2 was 50 tons compared with the 26 ton limit of OMI. This still is better than the 7000 ton limit of the 35 year old TOMS design, but the reduction in sensitivity is enough that monitoring of volcanic degassing is not possible with GOME-2. A comparison of a moderate degassing plume from Kilauea volcano in Hawaii is shown below:

OMI data on the left shows a clear source location over the south of the Big Island (Hawaii)and a connection to a SW trending plume while the GOME-2 data only hints that elevated SO_2 is present but it is not possible to identify the source.

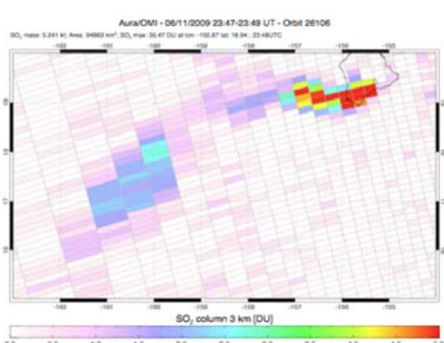

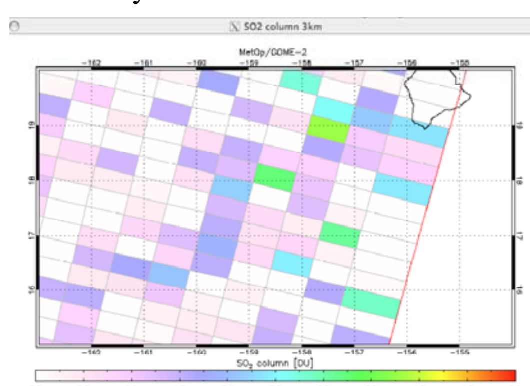

Another difference is in the retrieval of eruption clouds. Both instruments viewed the eruptions of Kasatochi in August 2008 and Sarychev in June 2009. The peak values and total SO_2 cloud masses measured by GOME-2 were about two-thirds of the OMI values. European researchers using a different retrieval method (DOAS) found similar differences between GOME-2 and SCIAMACHY data. It is clear that additional work is required before the GOME-2 data can be used quantitatively.

This difference does not significantly compromise the use of GOME-2 for detection of large volcanic clouds. However, the loss of degassing monitoring is significant for the DSS groups at USGS and for global volcano observatories.

Acknowledgements

This work could not have been successful without the assistance of the GSFC OMI Science Team; the SIPS team, who managed and operated the NRT OMSO2 data production; Marianne Guffanti of the USGS Volcano Hazards Program, who provided guidance and feedback on our data products; John Ewert of the Cascades Volcano Observatory; John Murray of the LaRC Aviation Weather program, who collaborated extensively on the Kasatochi eruption investigation; Lawrence Flynn of NOAA/ORA, who adapted GOME-2 TO3 data for volcano monitoring; Keith Evans of JCET, who maintained and improved the UMBC archival web site; and many others who contributed directly and indirectly.

Publications

Bani, P., C. Oppenheimer, V.I. Tsanev, S.A. Carn, S.J. Cronin, R. Crimp, J.A. Calkins, D. Charley, M. Lardy, and T.R. Roberts (2009). Surge in sulfur and halogen degassing from Ambrym volcano, Vanuatu, Bull. Volcanol., doi:10.1007/s00445-009-0293-7.

Carn, S.A., N.A. Krotkov, A.J. Krueger, K. Yang, and P.F. Levelt (2007). Sulfur dioxide emissions from Peruvian copper smelters detected by the Ozone Monitoring Instrument, Geophys. Res. Lett. 34, L09801, doi:10.1029/2006GL029020.

Carn, S.A., N.A. Krotkov, K. Yang, R.M. Hoff, A.J. Prata, A.J. Krueger, S.C. Loughlin, and P.F. Levelt (2007). Extended observations of volcanic SO2 and sulfate aerosol in the stratosphere, Atmos. Chem. Phys. Discuss., 7, 2857-2871. (http://www.atmos-chem-phys-discuss.net/7/2857/2007/acpd-7-2857-2007.html)

Carn, S.A., A.J. Krueger, N.A. Krotkov, S. Arellano, and K. Yang (2008). Daily monitoring of Ecuadorian volcanic degassing from space, J. Volcanol. Geotherm. Res., 176(1), 141-150, doi:10.1016/j.jvolgeores.2008.01.029.

Carn, S.A., A.J. Prata, and S. Karlsdóttir (2008). Circumpolar transport of a volcanic cloud from Hekla (Iceland). J. Geophys. Res., 113, D14311, doi:10.1029/2008JD009878.

Carn, S.A., A.J. Krueger, N.A. Krotkov, K. Yang, and K. Evans (2008). Tracking volcanic sulfur dioxide clouds for aviation hazard mitigation. Natural Hazards, doi:10.1007/s11069-008-9228-4

Carn, S.A., J.S. Pallister, L. Lara, J.W. Ewert, S. Watt, A.J. Prata, R.J. Thomas, and G. Villarosa (2009). The unexpected awakening of Chaitén volcano, Chile, EOS Trans. AGU, 90(24), 205-206.

Clerbaux, C., P.-F. Coheur, L. Clarisse, J. Hadji-Lazaro, D. Hurtmans, S. Turquety, K. Bowman, H. Worden, and S. A. Carn (2008). Measurements of SO2 profiles in volcanic plumes from the NASA Tropospheric Emission Spectrometer (TES). Geophys. Res. Lett., 35, L22807, doi:10.1029/2008GL035566.

Hughes, Eric. Using Horizontal Transport Characteristics to Infer an Emission Height Time Series of Volcanic SO_2. M.S. Thesis, University of Maryland, Baltimore County, May 2009.

Krotkov, N, A. , S. A. Carn, A.J. Krueger, P.K. Bhartia, and K. Yang, Band residual difference algorithm for retrieval of SO2 from the AURA Ozone Monitoring Instrument (OMI), IEEE Transactions on Geoscience and Remote Sensing, AURA special issue, 44(5), 1259-1266, doi:10.1109/TGRS.2005.861932, May 2006

Krotkov, N. A., B. McClure, R.R. Dickerson, S.A. Carn, C. Li, P.K. Bhartia, K. Yang, A.J. Krueger, Z. Li, P. Levelt, H. Chen, P. Wang, and D.R. Lu (2008), Validation of SO2 retrievals from the Ozone Monitoring Instrument (OMI) over NE China, J. Geophys. Res., 113, D16S40, doi:10.1029/2007JD008818.

Krueger, A., N. Krotkov, S. Carn, El Chichon: The genesis of volcanic sulfur dioxide monitoring from space, J. Volcanol. Geotherm. Res. (2008), http://dx.doi.org/10.1016/j.jvolgeores.2008.02.026; Journal of Volcanology and Geothermal Research, Volume 175, Issue 4, 20 August 2008, Pages 408-414. doi:10.1016/j.jvolgeores.2008.02.026.

Krueger, A. J., Kai Yang, Nickolay A. Krotkov, (2009). Enhanced monitoring of sulfur dioxide sources with hyperspectral UV sensors. Proc. SPIE, Vol. 7475, 74750Y (2009); doi:10.1117/12.830142.

Krueger, A. J., Nickolay A. Krotkov, Kai Yang, S. Carn, Gilberto Vicente, and Wilfrid Schroeder (2009), Applications of Satellite-Based Sulfur Dioxide Monitoring, IEEE Journal Of Selected Topics In Applied Earth Observations And Remote Sensing (JSTARS); doi: 10.1109/JSTARS.2009.2037334.

Krueger, A. J., Kai Yang, Nickolay A. Krotkov, (2009). Comparison of GOME-2 and OMI sulfur dioxide retrievals. Proc. Atmospheric Science Conference, Barcelona, Spain, 7-11 September 2009 (ESA SP-676, November 2009)

Martinsson, B.G., C.A.M. Brenninkmeijer, S.A. Carn, M. Hermann, K.-P. Heue, P.F.J. van Velthoven, and A. Zahn (2009). Influence of the 2008 Kasatochi volcanic eruption on sulfurous and carbonaceous aerosol constituents in the lower stratosphere. Geophys. Res. Lett., 36, L12813, doi:10.1029/2009GL038735.

Prata, A.J., S.A. Carn, A. Stohl, and J. Kerkmann (2007). Long range transport and fate of a stratospheric volcanic cloud from Soufriere Hills volcano, Montserrat, Atmos. Chem. Phys., 7, 5093-5103. (http://www.atmos-chem-phys.net/7/5093/2007/acp-7-5093-2007.html)

Prata, A.J., G.J.S. Bluth, C. Werner, V.J. Realmuto, S.A. Carn, and I.M. Watson (2009). Remote Sensing of Gas Emissions from Volcanoes, in Satellite Monitoring of Volcanoes: Spaceborne Images of the North Pacific, eds. K.G. Dean and J. Dehn (in press).

Sawyer, G.M., S.A. Carn, C. Oppenheimer, V.I. Tsanez, and M. Burton (2008). Investigation into magma degassing at Nyiragongo volcano, Democratic Republic of Congo. Geochem. Geophys. Geosyst., 9, Q02017, doi:10.1029/2007GC001829.

Thomas, H.E., I.M Watson, C. Kearney, S.A. Carn, and S.J. Murray (2009). A multi-sensor comparison of sulphur dioxide emissions from the 2005 eruption of Sierra Negra volcano, Galápagos Islands. Remote Sens. Environ., 113(6), 1331-1342, doi:10.1016/j.rse.2009.02.019.

Tupper, A., I. Itikarai, M. Richards, A.J. Prata, S.A. Carn, and D. Rosenfeld (2007). Facing the challenges of the International Airways Volcano Watch: the 2004/05 eruptions of Manam, Papua New Guinea, Weather and Forecasting 22(1), 175-191.

Yang, K., X. Liu, N.A. Krotkov, A.J. Krueger and S.A. Carn (2009). Estimating the altitude of volcanic sulfur dioxide plumes from space- borne hyper-spectral UV measurements, Geophys. Res. Lett., 36, L10803, doi:10.1029/2009GL038025.

Yang, K., N.A. Krotkov, A.J. Krueger, S.A. Carn, P.K. Bhartia, and P.F Levelt (2009). Improving retrieval of volcanic sulfur dioxide from backscattered UV satellite observations. Geophys. Res. Lett., 36, L03102, doi:10.1029/2008GL036036.

Yang, K., N.A. Krotkov, A.J. Krueger, S.A. Carn, P.K. Bhartia, and P.F. Levelt (2007). Retrieval of large volcanic SO2 columns from the Aura Ozone Monitoring Instrument (OMI): comparison and limitations. J. Geophys. Res., 112, D24S43, doi:10.1029/2007JD008825.

Yang, K., N. A. Krotkov, A. J. Krueger, S. A. Carn, P. K. Bhartia, and P. F. Levelt (2009), Improving retrieval of volcanic sulfur dioxide from backscattered UV satellite observations, Geophys. Res. Lett., 36, L03102, doi:10.1029/2008GL036036.